Ion dynamics in Ba-, Sr-, and Ca-doped La$_2$Mo$_2$O$_9$ from analysis of ac impedance

Santanu Basu · Himadri S. Maiti

Abstract Conductivity measurement on alkaline earth-doped La$_2$Mo$_2$O$_9$ is well documented, but the ion dynamic study of this material is scarcely reported. Alternating current impedance measurement of Ba-, Sr-, and Ca-doped La$_2$Mo$_2$O$_9$ in the light of ion dynamics has been discussed. The low-temperature regime, 250 °C to 500 °C, has been selected for study on the basis of frequency dispersion of conductivity as well as in terms of modulus formalism. The values of exponential parameter, s, of universal dielectric response and the stretching exponent, β, of Kohlrausch–Williams–Watts relation are evaluated from curve fitting. Scaling behavior of the doped materials has also been investigated. Temperature dependence of such parameters is checked and is interpreted for the plausible mechanism of ionic motion in the material at low temperature.

Keywords Ionic conduction · Lanthanum molybdate · Ion dynamics · Modulus formalism · Scaling

Introduction

Electrical relaxation in liquids and glasses with high concentration of mobile ions is well manifested [1]. The power law analyses of alternating current (ac) conductivity data are proven to be a highly informative approach. Such study has also been extended to different crystalline materials which are predominantly ionic in nature [2–10].

In recent years, an oxygen ionic conductor, reported by Lacorre et al. [11, 12], namely, lanthanum molybdate

La$_2$Mo$_2$O$_9$, has attracted much attention due to its high ionic conductivity at medium temperature (0.06 S/cm at 800 °C). Although a large number of work has already been published on pure and doped La$_2$Mo$_2$O$_9$ [13–22], little work [23, 24] has been done on the conductivity relaxation in La$_2$Mo$_2$O$_9$.

Due to the ionic radii, alkaline earth substitutions (Ba, Sr, and Ca) are found to be appropriate for La^{+3} site. The effect of such aliovalent substitutions has already been reported in our earlier work [18]. Although ionic conductivity of these materials is well documented, the ion dynamics of these materials are scarcely reported [23]. It has been reported that Ca and Sr doping results in the formation of secondary impurity phases like (Ca,Sr)MoO$_4$ [19] which may influence the conductivity of La$_2$Mo$_2$O$_9$. Our compositions are free from such impurities phases; therefore, conductivity of substituted La$_2$Mo$_2$O$_9$ reported here do not have any contribution from impurity phases. In this work, we have extended the ion dynamics study on alkaline earth substituted (Ba, Sr, and Ca) La$_2$Mo$_2$O$_9$ by means of different representations of ac impedance data such as frequency dispersion of real part of conductivity, modulus formalism, and scaling behavior. Scaling behavior has also been studied to find out whether the mechanism of ion conduction depends on different parameters such as temperature and composition.

Experimental

The substituted La$_2$Mo$_2$O$_9$ compositions were prepared by citrate nitrate auto-combustion technique. Lanthanum nitrate hexahydrate [La(NO$_3$)$_3$·6H$_2$O,99%], ammonium heptamolybdate [(NH$_4$)$_6$Mo$_7$O$_{24}$·4H$_2$O,99%], citric acid monohydrate, distilled water, and nitrates of corresponding

S. Basu (✉) · H. S. Maiti
Central Glass and Ceramic Research Institute,
Kolkata 700032, India
e-mail: santanubasu72@hotmail.com

dopants (Ba, Ca, and Sr) were used for the synthesis. The synthesis procedure is described in details elsewhere [25].

The calcined powders were subjected to uniaxial compaction and then sintered between 1,000 °C and 1,150 °C depending on the compositions to achieve densities more than 96% of theoretical density. X-ray diffraction pattern of these sintered materials has proven the non-existence of impurity phases such as $CaMoO_4$ or $SrMoO_4$.

Two probe ac impedance measurements were conducted on sintered, electroded samples in the frequency range 0.1 Hz to 10 MHz using a Solartron frequency response analyzer (FRA 1260) in the temperature range 200–500 °C. The impedance data were analyzed using Z-VIEW software.

The value of exponential parameter, s, were evaluated by nonlinear curve fitting using Origin® software. The goodness of the fitting for each cases was greater than 0.95. Stretching exponent β was evaluated using the method described by Sidebottom et al. [9].

Results and discussion

Measurement of the ac conductivity, σ, generally shows a frequency dispersion, i.e., the real part of ac conductivity $\sigma'(\omega)$ depends on the angular frequency ω. Large span of conductivity spectroscopy over decades on the frequency scale, ranging from 10^{-2} Hz to more than 10^{14} Hz, reveals an opportunity to study the motion of charged particles ions taking place at very different timescales; moreover, their elementary hopping mechanism can also be resolved. Therefore, Funke and Cramer [26] logically denoted ac conductivity as an extremely powerful "microscope in time."

The frequency dispersion of real part of ac conductivity in air for the composition $La_{1.94}Ba_{0.06}Mo_2O_{9-\delta}$ is shown in Fig. 1. Since grain boundary effects are not of interest here, such low frequency data points are omitted [27]. Each curve shown in the Fig. 1 consists of a low-frequency plateau which corresponds to the direct current (dc) conductivity and a high-frequency dispersive region, which corresponds to the ac conductivity. The low-frequency plateau is a distinct nature of hopping models. At high frequencies, the electric field changes its sign so fast that the consecutive hops do not fit into a timescale.

The conductivity spectrum of ionic conductors has been found to exhibit universal power law behavior [28], i.e.,

$$\sigma' = \sigma(0) + A(\omega)^s \tag{1}$$

where $\sigma(0)$ is termed as the dc conductivity and s is the power law exponent. Such behavior was denoted as universal dielectric response (UDR) by Jonscher [28].
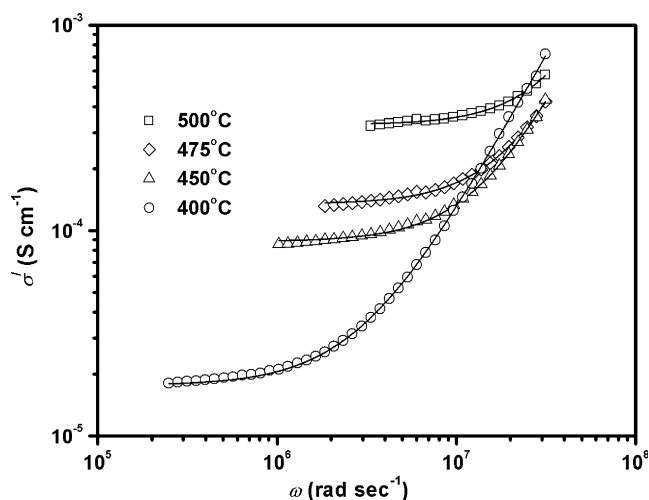

Fig. 1 Temperature dependence of frequency dispersion of real part of conductivity of $(La_{0.97}Ba_{0.03})_2Mo_2O_9$

Almond and West [29] have suggested that ac conductivity data such as the power law exponent reveal important information on the ion dynamics. Thus, Eq. 1 is fitted on the above curves to evaluate the exponential constant s.

The nature of the curves for frequency dispersion of conductivity of 3 mol% Ca- and Sr-substituted $La_2Mo_2O_9$ composition at 400 °C is very similar to that of 3 mol% Ba-substituted composition as described in Fig. 1. Other alkaline earth-doped compositions show similar nature of frequency dispersion of conductivity, and their corresponding s values are evaluated. Table 1 describes the exponential parameter s for different alkaline earth-doped compositions at different temperatures, and it is found to vary from 0.32 to 0.51. It is evident that there is no systematic dependence of s on temperature, but with increase of Ba content, the value of s increases, indicating interaction of mobile ions which increases as their density increases with the increase of dopant concentration. Such observation is also evident for its Ca and Sr counterparts. Conductivity values at 400 °C, obtained from the complex plane impedance plot, are compared (Table 1) with $\sigma(0)$ obtained from the fitting of Eq. 1. Proximity of these values validates fitting.

The electrical modulus formalism was introduced in 1972 by Macedo et al. [30] in an effort to simplify analysis of impedance data. The electrical modulus is the quantity formed from reciprocating the complex dielectric permittivity:

$$M^* = 1/\varepsilon^* = M' + iM'' \tag{2}$$

If the charges of the opposite sign are instantaneously placed on opposite faces of an ion conductor at time 0 and then maintained at a constant value, then there will arise inside an electrical field E that in time will decay to 0 due to migration of the mobile ions.

Table 1 Electric field relaxation parameters and ionic conductivity of alkaline earth-substituted La$_2$Mo$_2$O$_9$

Substitutions	s				β				σ$_{400\,°C}$ (Scm^{-1})	
	Temperature (°C)				Temperature (°C)				Nyquist	UDR
	300	325	350	400	300	325	350	400		
Pure	0.33±0.02	0.32±0.05	0.37±0.02	0.36±0.01	0.69±0.02	0.68±0.01	0.66±0.02	0.68±0.01	6.70±0.01 × 10^{-6}	6.58±0.02 × 10^{-6}
3% Ba	0.38±0.12	0.39±0.01	0.42±0.12	0.44±0.06	0.62±0.01	0.63±0.02	0.59±0.02	0.60±0.02	7.65±0.03 × 10^{-6}	7.21±0.02 × 10^{-6}
5% Ba	0.41±0.03	0.40±0.15	0.43±0.05	0.45±0.02	0.60±0.03	0.61±0.01	0.59±0.01	0.58±0.02	7.22±0.01 × 10^{-6}	6.84±0.02 × 10^{-6}
8% Ba	0.43±0.03	0.45±0.12	0.44±0.14	0.46±0.03	0.58±0.03	0.57±0.01	0.58±0.03	0.56±0.02	6.95±0.01 × 10^{-6}	6.81±0.01 × 10^{-6}
3% Sr	0.44±0.04	0.45±0.05	0.45±0.12	0.43±0.02	0.57±0.02	0.56±0.03	0.57±0.02	0.58±0.01	6.97±0.04 × 10^{-6}	6.72±0.01 × 10^{-6}
5% Sr	0.46±0.02	0.47±0.07	0.46±0.03	0.47±0.03	0.55±0.04	0.55±0.02	0.54±0.01	0.55±0.02	6.88±0.03 × 10^{-6}	6.69±0.01 × 10^{-6}
8% Sr	0.47±0.13	0.49±0.02	0.48±0.01	0.49±0.05	0.53±0.02	0.52±0.02	0.53±0.02	0.52±0.03	6.78±0.02 × 10^{-6}	6.63±0.02 × 10^{-6}
3% Ca	0.42±0.06	0.43±0.13	0.40±0.04	0.43±0.03	0.59±0.02	0.60±0.03	0.61±0.04	0.61±0.02	6.71±0.03 × 10^{-6}	6.56±0.01 × 10^{-6}
5% Ca	0.43±0.01	0.46±0.08	0.45±0.15	0.47±0.02	0.57±0.01	0.56±0.01	0.57±0.02	0.56±0.02	6.70±0.02 × 10^{-6}	6.57±0.03 × 10^{-6}
8% Ca	0.48±0.05	0.47±0.05	0.51±0.08	0.48±0.02	0.53±0.01	0.54±0.03	0.52±0.02	0.53±0.03	6.68±0.02 × 10^{-6}	6.52±0.01 × 10^{-6}

The decay may be described in the time domain by:

$$E(t) = E(0)\phi(t) \tag{3}$$

where $\phi(t)$ is a decay function which can be written in general from as described by Kohlrausch–Williams–Watts (KWW):

$$\phi(t) = \exp\left[-(t/\tau)^\beta\right] \tag{4}$$

where τ is temperature-dependent relaxation time constant and β is Kohlrausch exponent. $\phi(t)$ can be interpreted as resulting from the sum of many exponential decays weighted by a distribution of individual relaxation times for which the small value of β expresses larger distribution of relaxation times [30]. Moynihan et al. [1] introduced the KWW relaxation function in an empirical manner to characterize the width of the $M^{//}$ peaks in terms of stretching component β. The smaller the value of β, the broader is the peak and the larger is the deviation of the relaxation with respect to a Debye-type relaxation.

Modulus formalism is used to analyze the dielectric behavior of different doped La$_2$Mo$_2$O$_9$. Temperature and frequency dependence of imaginary part of modulus in air for the composition La$_{1.94}$Ba$_{0.06}$Mo$_2$O$_{9\,-\,\delta}$ is shown in Fig. 2. The $M^{//}$ peak shifts toward the high frequency with increase in temperature. The shift of frequency maxima may be due to the distribution of attempt frequencies for the barrier crossover or flight distances following the crossover or a distribution of attempt frequency. The full width half height, i.e., the shape of the curves, does not change considerably with temperature; thus, distribution of relaxation times for ions in the La$_{1.94}$Ba$_{0.06}$Mo$_2$O$_{9\,-\,\delta}$ remains independent of temperature.

The results of these two very useful methods of presenting ion dynamics, namely, the complex electrical

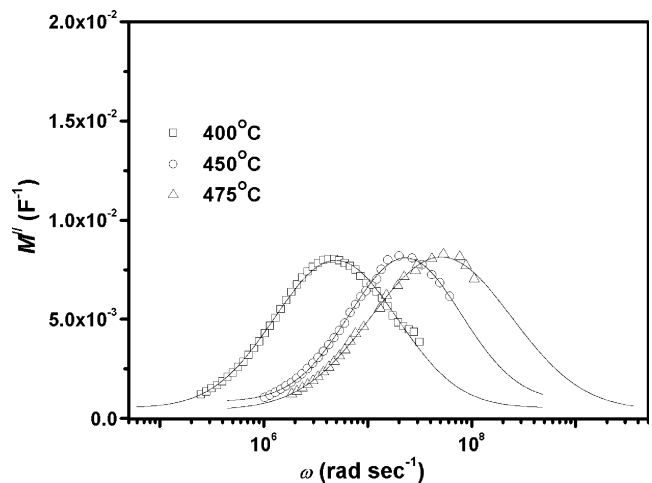**Fig. 2** Temperature dependence of imaginary part of modulus of (La$_{0.97}$Ba$_{0.03}$)$_2$Mo$_2$O$_9$

modulus formalism and analysis in terms of the complex conductivity, seem to contradict when explaining ion transport [30]. The apparent contradiction between the M''- and σ'-based methods can be resolved when scaling method is introduced in the system [31]. Scaling ac conductivities into a single master curve has been tried by several researchers. It is a common practice to scale ordinate of temperature- and composition-dependent curves of $\sigma(\omega)$ by $\sigma(\omega)/\sigma_{dc}$. Roling [32] scaled abscissa by $f/(\sigma_{dc}T)$ or by $f_x/(\sigma_{dc}T)$, x being the composition. Sidebottom [33] and Schroeder and Dyre [34] scaled abscissa by $f\varepsilon_0\Delta\varepsilon/\sigma_{dc}$. However, it is found to be best to scale the ac data by the plot of logarithmic $\sigma(\omega)/\sigma_{dc}$ as a function of logarithmic $f/f_r(= 2\pi f \in_0 \Delta \in /\sigma_{dc})$ [35] because normalized log–log curves of $\sigma(\omega)$ of various ionic conductors upturn from zero of the ordinate near zero of the abscissa with increasing frequencies. Patel and Martain [36] plotted $\sigma(\omega)/\sigma_{dc}$ as a function of logarithmic f/f_p (f_p being the frequency of M'' peak maximum, which is similar to f_r).

Scaling study has been made on the different substituted $La_2Mo_2O_9$ compositions. Figure 3 shows the scaling behavior of frequency dispersion of conductivity with different Ba-substituted compositions in air atmosphere at 400°C. The single master curve is observed.

At different temperatures, the scaling behavior remains the same. Real part of conductivity data when scaled for 3 mol% Ba-substituted $La_2Mo_2O_9$ at different temperatures obtained single master curve as shown in Fig. 4. All the curves collapsed into a single master curve. Thus, the mechanism of ion conduction does not alter with temperature [17]. Similar nature is observed for Sr- and Ca-substituted compositions also. These observations suggest that the conductivity relaxation mechanism is temperature-independent.
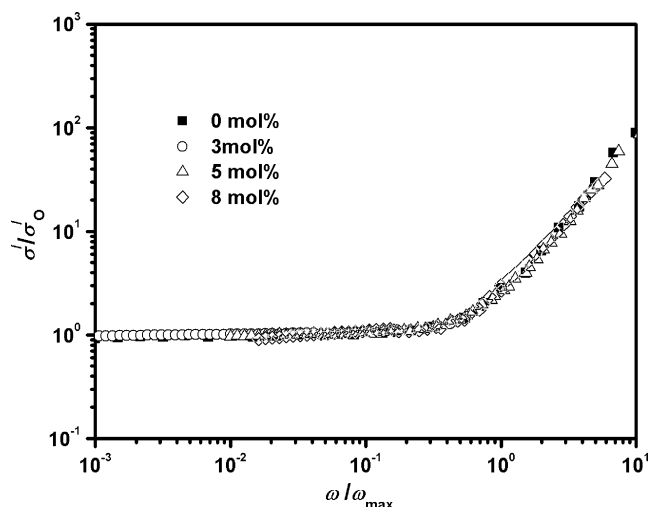

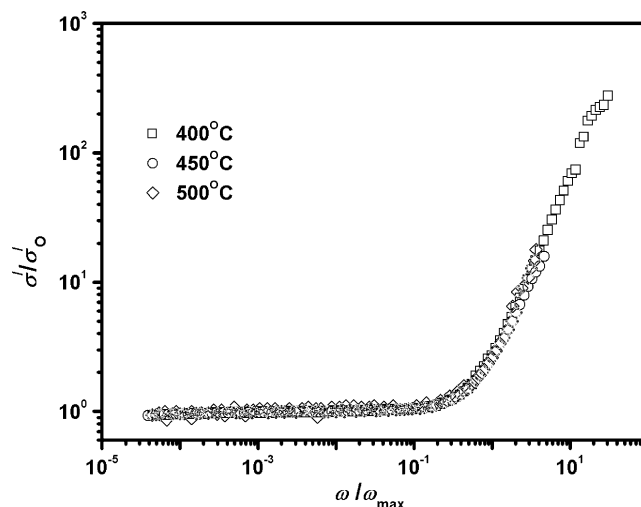**Fig. 4** Scaled real part of conductivity in 3 mol% Ba-substituted $La_2Mo_2O_9$ at different temperatures

In Fig. 5, modulus scaling of different dopant compositions are compared, and it is noticeable that single master curve can describe all the compositions irrespective of the dopant cation and their concentrations. This indicates that the mechanism of ionic motion remains the same with change of alkaline earth dopant cation and their concentrations under the experimental limit. Even the pure high-temperature β form and its mixture with low-temperature α form do not show any alteration, as all the Ba-substituted compositions fully stabilize the high-temperature β form at room temperature, whereas for its Ca and Sr counterparts, only partial stabilization is observed for low to moderate concentration [18].

The non-symmetric behavior of the M''/M''_{max} curves can be described by the KWW function $\Phi(t)$, which represents the relaxation time distribution in the ionic
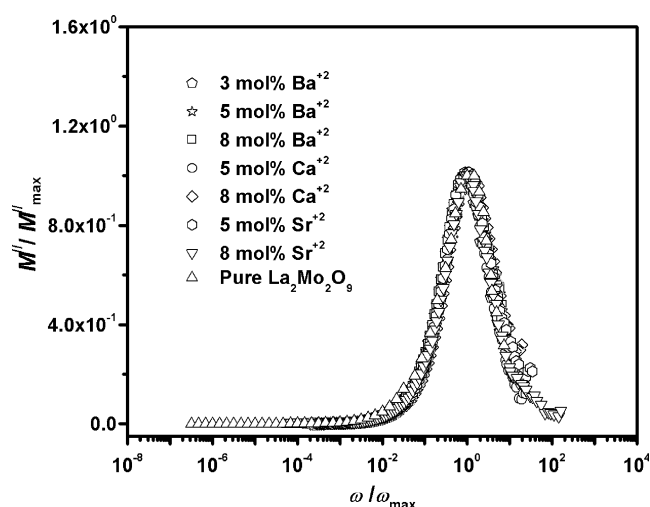

Fig. 3 Scaled real part of conductivity of different mol% Ba-substituted as well as pure $La_2Mo_2O_9$ at 400°C

Fig. 5 Scaled imaginary part of electrical modulus of different alkaline earth cation-substituted as well as pure $La_2Mo_2O_9$ at 400°C

conduction [8]. From the $M^{//}$ versus log ω curves (Fig. 2), the value of β is evaluated using the method described by Sidebottom et al. [9]. The Kohlrausch exponent β is calculated for different compositions for different temperatures and is shown in Table 1. From Table 1, it can be observed that the stretch exponent β decreases with an increase of substitution concentration, implying gradual deviation from the Debye-like behavior. Energetically three different structural oxygen positions in the pure $La_2Mo_2O_9$ itself [12] may influence the transportation from one O site to the other; hence, the ionic transport is not an isolated event but rather a time-dependent motion. With the introduction of aliovalent substitutions, interaction of mobile ions increases and thus results in a larger distribution of relaxation time.

It is noticeable that values of β are not dependent on temperatures. We have already discussed earlier that the value of s is also temperature-independent. Thus, we may conclude that s and β are related. According to coupling model introduced by Ngai et al. [37], stretch parameter β and power law component s of conductivity spectra correlated by the relation $\beta = 1 - s$. In proposition to this model, correlation between ions might take place after a critical time, t_c; the relaxation rate would be a constant at very short time. After the critical time, the relaxation would slow down and the time-dependent relaxation is a KWW function. The calculated $\beta_{cal}(=1-s)$ is found to decrease gradually with an increase of substitution concentration (as s increases with substitution, it is oblivious) as the β obtained from the experimental data fitting (Table 1) also shows a similar trend, but are little higher than β_{cal}, which is a recognized fact in various ionic conductors [9, 38].

Conclusions

Ion dynamics of alkaline earth-substituted $La_2Mo_2O_9$ have been discussed in terms of modulus formalism and frequency dispersion of conductivity. The value of exponential constant s was evaluated and found to vary from 0.32 to 0.51. There is no systematic dependence of s on temperature. Increase of Ba content increases the value of s and indicates a growing interaction of mobile ions as their density increases with increase of dopant. Such observation also appears for Ca- and Sr-doped compositions. The β parameter and the power law exponent s were found to satisfy the relation $\beta = 1 - s$. The plot of scaled power law spectra of $\log(\sigma^{/}/\sigma_0^{/})$ versus $\log(\omega/\omega_{max})$ at different temperatures suggested that the conductivity relaxation mechanism is temperature-independent, while superposition of the plot of scaled modulus spectra $M^{//}/M_{max}^{//}$ versus $\log(\omega/\omega_{max})$ for various substituted compositions indicates composition independence of the substituted $La_2Mo_2O_9$.

References

1. Moynihan CT, Boesch LP, Laberage NL (1973) Phys Chem Glasses 14:122
2. Almond DP, Hunter CC, West AR (1984) J Mater Sci 19:3236
3. Funke K, Roling B, Lange M (1998) Solid State Ionics 105:195
4. Hairetdinov F, Uvarov NF, Patel HK, Martin SW (1994) Phys Rev B 50:13259
5. Martin W, Angell CA (1986) J Non-Cryst Solids 83:185
6. Ngai KL, Mundy JN, Jain H, Kanert O, Balzer-Jollenbeck G (1989) Phys Rev B 39:6169
7. Jain H, Krishnaswami S (1998) Solid State Ionics 105:129
8. Roling B, Happe A, Funke K, Ingram MD (1997) Phys Rev Lett 78:2160
9. Sidebottom DL, Green PF, Brow RK (1995) J Non-Cryst Solids 183:151
10. Leon C, Lucia ML, Santamaria J, Paris MA, Sanz J, Varez A (1996) Phys Rev B 54:184
11. Lacorre P, Goutenoire F, Bohnke O, Retoux R, Laligant Y (2000) Chem Mater 12:2575
12. Lacorre P, Goutenoire F, Bohnke O, Retoux R, Laligant Y (2000) Nature 404:856
13. Goutenoire F, Isnard O, Suard E, Bohnke O, Laligant Y, Retoux R, Lacorre P (2001) J Mater Chem 11:119
14. Lacorre P, Retoux R (1997) J Solid State Chem 132:443
15. Wang XP, Fang QF, Li ZS, Zhang GG, Yi ZG (2002) Appl Phys Lett 81:3434
16. Collado JA, Aranda MAG, Cabeza A, Olivera-Pastor P, Bruque S (2002) J Solid State Chem 167:80
17. Georges S, Goutenoire F, Laligant Y, Lacorre P (2003) J Mater Chem 13:2317
18. Basu S, Devi PS, Maiti HS (2004) Appl Phys Lett 85:3486
19. Subasri R, Matusch D, Nafe H, Aldinger F (2004) J Eur Ceram Soc 24:129
20. Hayward SA, Redfern SAT (2004) J Phys Condens Matter 16:3571
21. Khadasheva ZS, Venskovskii NU, Safrenko MG, Mosunov AV, Politova ED, Yu SS (2002) Inorg Mater 38:1168
22. Basu S, Devi PS, Maiti HS (2005) J Electrochem Soc 152:A2143
23. Basu S, Maiti HS (2009) Ionics. doi:10.1007/s11581-009-0358-9
24. Basu S, Maiti HS (2009) J Electrochem Soc 156:P114
25. Basu S, Sujatha Devi P, Maiti HS, Lee Y, Hanson JC (2006) J Mater Res 21:1133
26. Funke K, Cramer C (1997) Curr Opin Solid State Mater Sci 2:483
27. Nowick AS, Vaysleyb AV, Kuskovsky I (1998) Phys Rev B 58 (13):8398
28. Jonscher AK (1977) Nature 67:673
29. Almond DP, West AR (1983) Solid State Ionics 9-10:277
30. Mecado PB, Moynihan CT, Bose R (1972) Phys Chem Glasses 13:171
31. Simmons JH, Elterman PB, Simmons CJ, Mohr RK (1979) J Am Ceram Soc 62:158
32. Roling B (1998) Solid State Ionics 105:185
33. Sidebottom DL (1999) Phys Rev Lett 82:3653
34. Schroeder TB, Dyre JC (2000) Phys Rev Lett 84:310
35. Doi A (2006) J Non-Cryst Solids 352:777
36. Patel HK, Martin SW (1992) Phys Rev B 45:10292
37. Ngai KL, Randell RN, Jain H (1984) Phys Rev B 30:2133
38. Arakawa S, Sano J, Hayashi S (2000) J Am Ceram Soc 83:2705